



# Survey study of mercury determination in detonation nanodiamonds by pyrolysis flameless atomic absorption spectroscopy

D.S. Volkov <sup>\*</sup>, M.A. Proskurnin, M.V. Korobov

Chemistry Department of M.V. Lomonosov Moscow State University, Leninskie Gory, 1-3, GSP-1, Moscow 119991, Russia  
Analytical Centre, Chemistry Department of M.V. Lomonosov Moscow State University, Leninskie Gory, 1-3, GSP-1, Moscow 119991, Russia

## ARTICLE INFO

### Article history:

Received 19 November 2013  
Received in revised form 6 August 2014  
Accepted 31 August 2014  
Available online 6 September 2014

### Keywords:

Nanodiamond  
Nanoparticles  
Impurity characterization

## ABSTRACT

A set of 20 commercially available nanodiamond samples of eight manufacturers of various countries, which are most frequently used in basic and applied studies, was analyzed for the concentration of Hg. Conditions of mercury determination by flameless atomic absorption spectroscopy with thermal sample decomposition (pyrolysis) at 800 °C were proposed and confirmed by wavelength-dispersive X-ray fluorescence analysis. It was found that nanodiamonds have a significant diversity of amounts of mercury, from 20 µg/kg to higher than 0.7 g/kg. Thus, the need to control Hg impurity in nanodiamonds, especially for biological and medical research, was demonstrated. The precision of flameless pyrolysis atomic absorption determination of mercury in nanodiamonds is discussed.

© 2014 Elsevier B.V. All rights reserved.

## 1. Introduction

Unique properties of new allotropic forms of carbon—fullerenes, nanotubes, and nanodiamonds—find various applications in state-of-the-art branches of science and technology. Nanodiamonds (NDs) are very promising materials, especially for biomedical applications [1], catalysis [2,3], and as new sorbents [4–7]. They can be used as fluorescent agents [8–10] in clinical diagnostics, as platforms for drug delivery [11, 12], as enterosorbents, diagnostic sensors, in cellular surgery, anticancer therapy, and many other areas [1]. ND biocompatibility has been intensively investigated recently [13]. Low ND toxicity was shown for neurons [14], stem cells [15], pulmonary epithelium [16,17], blood cells [18], fibroblasts [16,17], ovary tissues [19] etc.

In fact, ND properties that are crucial for medical and high technological uses (aggregate size, surface groups, optical and colloidal properties, etc.) depend on their production and purification technology. In particular, it is very important to know the impurity composition precisely because some chemical elements may be hazardous even in trace quantities, especially when they are present in nanomaterials. Impurities in detonation NDs have various nature like metal-oxide micro-particles, carbides, silicon dioxide, or insoluble salts as well as cations and anions adsorbed at the ND surface [20–22]. These impurities appear due to the interaction of the blast wave with the walls of the detonation reaction chamber (Fe and Cr) or from the explosion initiation (Cu, Pb, and Hg) [21], and adsorbed [23] on already formed nanodiamonds

from liquids (acids and water) used for their isolation from the detonation-chamber charge [22,24].

Currently, traceability is one of the most topical problems of ND technology [25]. Development of analytical-monitoring techniques is the first crucial step to make ND properties traceable and to improve and advance the required technologies.

The first step is to check the content of metals and nonmetal elements, as even in small amounts, they can have a significant impact on the biological and catalytic processes. In addition, they also change the properties of the nanodiamonds, such as their thermal and oxidative resistance [26,27]. Until now, not much attention was focused on multielement chemical analysis of NDs, although its importance was declared from the very start of ND research. Probably, this situation is due to a need to strictly monitor the purity of the preparation, while ND traceability is still not achieved [25]. Recently, Nesterenko has presented a rather deep study of the elemental composition of NDs using inductively-coupled plasma mass-spectrometry [28] and we made a survey of the most common types of NDs using ICP-AES [29]. Still, mercury determination in NDs is topical due to its low least tolerable amounts. However, to understand the problem in full, a large variety of NDs is required. Thus, the aim of this study is to make a survey study of mercury in NDs for the most common commercially available ND products (Table 1).

Another thing is to select a method for such a survey, and there is still a need for traceable and reliable analytical tools for ND impurity characterization. One of the most common methods for the determination of trace mercury is atomic absorption spectrometry (AAS) due to its high precision and availability, which is better than ICP-AES, and this method provides much simpler procedures—compared to ICP-MS—giving reliable results. However, its widespread variant, cold-vapor

Abbreviations: ND, nanodiamond; FPAAS, flameless AAS coupled with pyrolysis WDXRF; WDXRF, wavelength dispersive X-ray fluorescence.

<sup>\*</sup> Corresponding author. Tel.: +7 495 9393514.

E-mail address: [dmsvolkov@gmail.com](mailto:dmsvolkov@gmail.com) (D.S. Volkov).

**Table 1**  
Nanodiamonds used in the survey.

| NDs product name             | Description  | Manufacturer   |
|------------------------------|--|--|
| RUDDM (1) <sup>a</sup>       | Modified nanodiamond material of RUDDM grade, fraction 0–150   | “Real-Dzerzhinsk” Ltd., Dzerzhinsk, Russia   |
| RUDDM (2) <sup>a</sup>       |  |  |
| RUDDM (3) <sup>a</sup>       |  |  |
| RUDDM non-fractionated       | Modified nanodiamond material of RUDDM grade, non-fractionated | PlasmaChem GmbH, Germany   |
| RDDM                         | Modified nanodiamond material of RDDM grade, fraction 0–0.125  |  |
| SDND                         | Single-digit NanoDiamonds                                      |  |
| WND                          | WND  |  |
| NanoPure-GO1                 | NanoPure-GO1   |  |
| NanoAmando 2009 <sup>a</sup> | NanoAmando   | NanoCarbon Research Institute Co., Ltd., Japan   |
| NanoAmando 2012 <sup>a</sup> |  |  |
| UDA-TAN                      | DNA-TAN  | “Tekhnolog” Special Construction-Technological Bureau, St. Petersburg, Russia  |
| UDA-STP                      | DNA-STP  |  |
| UDAG-S                       | UDAG-S, diamond-carbon powder                                  | The Laboratory of ultradispersed diamonds of Joint Stock Company Federal Research and Production Center ALTAL, Biysk, Russia |
| UDA-S                        | UDA-S, ultradispersed diamond powder                           |  |
| UDA-S-GO                     | UDA-S-GO, ultradispersed diamond powder of deep purification   |  |
| UDA-SP                       | UDA-SP, ultradispersed diamonds                                |  |
| UDA-GO-SP                    | UDA-GO-SP, deep purified ultradispersed diamonds               |  |
| UDA-GO-SP-M1                 | UDA-GO-SP-M1, modified ultradispersed diamonds, type M1        | JSC “SINTA”, Minsk, Republic of Belarus  |
| UDA-GO-SP-M2                 | UDA-GO-SP-M2, modified ultradispersed diamonds, type M2        |  |
| UDD-Alit                     | UDD, Ultra Dispersed Diamond powder                            |  |
| UDD-NanoGroup                | UDD, Ultra Dispersed Diamond                                   | “ALIT”, Kiev, Ukraine  |
|                              |  | “NanoGroup Co.” Prague, Czech Republic   |

<sup>a</sup> Different lots of one trademark obtained at different times.

AAS based on atomic absorption of  $\text{Hg}^0$  reduced from  $\text{Hg}^{2+}$  [30] is not suitable well when a direct analysis of solid matrices is required. Flameless AAS coupled with pyrolysis (FPAAS) is a well-known and advantageous AAS technique, very specific and sensitive to Hg and featuring no sample pretreatment and free from matrix interferences. This technique is based on the pyrolysis of the sample in a combustion tube at 750–1000 °C under an air or oxygen atmosphere and subsequent detection of Hg vapor by AAS [31,32]. It was used for direct determination of mercury in various samples: geological materials [33], soils, sediments [31], oil [34], biological objects [32,35,36], foodstuffs [37], medical materials [38,39], and cigarettes [40].

Thus, to fulfill the aim of this study, we selected flameless pyrolysis AAS for the survey quantification of mercury in nanodiamonds with minimum sample preparation.

## 2. Material and methods

The measurement results are presented as mean values with confidence intervals in accordance with the requirements for the competence of testing and calibration laboratories, ISO/IEC 17025:2005 [41]. Calibration parameters were calculated according to the IUPAC 1998 recommendations for the presentation of the results of chemical analysis [42].

### 2.1. Nanodiamond samples

Commercially available NDs were used throughout. Trademarks, their product names, and manufacturers are listed in Table 1. All NDs are dry powders except SDND, WND, and Nanopure GO-1 materials. The latter samples were aqueous dispersions, which were dried in a heating oven.  $\text{SiO}_2$  thin powder (silica gel) from Reakhim, Russia, and Russian State Reference Material of mercury solution (GSO 7343-96, Hg(II) content  $(1.00 \pm 0.05)$  g/L), were used for preparing calibration mixtures in 30-ml polypropylene vessels.

The control of trueness in accordance with the requirements of ISO 5725:1994 [43] was made using a certified reference material—Russian State Reference Material of a soil sample with a certified mercury content  $(0.4 \pm 0.1)$  ppm. Deionized water ( $18.2 \text{ M}\Omega \times \text{cm}$ ) from a Milli-Q Academic System (Millipore, France) was used throughout for solution preparations.

### 2.2. Equipment

An RA-915+ Mercury Analyzer (Ohio Lumex Co., Russia) with a RP-91C pyrolysis accessory (Lumex, Russia) was used for FPAAS mercury determination in dry nanodiamond samples. RA-915+ is a portable multifunctional atomic absorption spectrometer with Zeeman high-frequency modulation of polarization for background correction [36, 44–46]. RP-91C is intended as an accessory for thermal decomposition of solid samples at 800 °C under air atmosphere and the transformation of bound Hg from ionic to atomic species for subsequent determination with a RA-915+ analyzer. The attested detection limit of this analytical system is  $0.5 \mu\text{g/kg}$  (0.5 ppb) at 200 mg of sample [47]. The analysis time is 3 min per a single determination including sample weighing, combustion, and cooling combustion tube. Typical decomposition time was about 15–40 s.

A HG63 Moisture Analyzer (Mettler-Toledo AG Laboratory & Weighing Technologies, Switzerland) was used for water content determination. Samples of 1 g were used for analysis; drying temperature was at 105 °C. The automatic “weight loss per unit of time” switch-off criterion was used for measurements, when drying is automatically ended as soon as the mean weight loss ( $\Delta g$  in mg) per unit of time ( $\Delta t$  in seconds) drops below a preset value. A SNOL 20/300 heating oven (Snol-Term Ltd., Russia) was used for the evaporation of ND (SDND) aqueous dispersions. An Ohaus Explorer Pro Analytical Balance (Ohaus, Switzerland; max weight 210 g, repeatability std. dev. 0.1 mg) was used for weighing dry powder samples. Automatic Eppendorf Research pipettes (Eppendorf International, Germany) and A-class volumetric flasks (ISOLAB, Germany) from borosilicate glass with a volume of  $(50.000 \pm 0.060)$  ml were used for diluted mercury solution preparation.

To confirm the presence of high amounts of Hg in ND samples, we measured the X-ray spectra of ND powders in helium mode. A Thermo Scientific ARL Advant’x 4200 wavelength-dispersive X-ray spectrometer (Thermo Scientific, Switzerland) with OXSAS X-ray Fluorescence Analytical Software (Thermo Scientific) was used for the measurements of X-ray fluorescence spectra. To implement this, the samples with Hg contents of more than 0.1 ppm, according to FPAAS (UDA-S, UDA-S-GO, and UDAG-S), and a sample with a low Hg content (RUDDM non-fractionated) were placed into polypropylene cells with Spectrolene-film window (6  $\mu\text{m}$ , Fisher Scientific), the cells were placed into the sample holder, covered, and introduced into the XRF spectrometer.

The fluorescence of the Hg  $L_{\alpha}$  line was measured. Measurement conditions are summarized in Table 2.

### 2.3. Procedures

#### 2.3.1. Procedure 1. The calibration

Modeling calibration mixtures were made from mercury-free  $\text{SiO}_2$  powder and the solutions with precisely known Hg(II) content. To do this, 5 ml of the GSO 7343–96 mercury solution was placed into a 50-ml volumetric flask and diluted (stock Solution 1 with a mercury concentration of 100 ppm). Next, 5 ml of Solution 1 was placed into a 50-ml volumetric flask and diluted (stock Solution 2 with a mercury concentration of 10 ppm). Next, the necessary amount of  $\text{SiO}_2$  (see Table 3) was placed into polypropylene vessels, and the necessary volumes of the stock solutions were added exactly into the powder. Moreover, 10.000 g of clean, mercury-free  $\text{SiO}_2$  powder was placed into an additional vessel (the blank mixture). Next, all powders in vessels, including blank, were put into the heating oven and dried at 35 °C for 1 h. Next, vessels were closed and intensively mixed by handling shaking for 1 min.

Weighed portions of every calibration mixtures (ca. 100 mg) were placed into a quartz combustion boat, and after the background signal recording was started, the boat was inserted into the oven of the RP-91C accessory. The signal was measured until all the mercury evaporated and the signal returned to the background level. Series of 10 replicates were made for the blank mixture and 3 replicates for all the test samples.

#### 2.3.2. Procedure 2. Mercury determination in samples with low Hg content

Weighed portions (50–300 mg) were placed into a quartz combustion boat and the signal was measured as described for the calibration above. A series of 3 replicates were made for all the samples (except those diluted with  $\text{SiO}_2$ ) using different weights, e.g. 100, 200, and 300 mg of the sample.

#### 2.3.3. Procedure 3. Mercury determination in samples with high Hg content

Samples with high mercury content (>10 ppm) were diluted by mixing with  $\text{SiO}_2$  powder. To do this, the necessary amount of  $\text{SiO}_2$  and NDs was mixed as described in Table 4. Next, each ND– $\text{SiO}_2$  mixture and blank  $\text{SiO}_2$  was measured 6 times as described above for samples with low Hg content.

#### 2.3.4. Procedure 4. Moisture content determination

Moisture contents in all commercial ND were determined by a thermogravimetry moisture analyzer. For this part of each sample was placed into the analyzer, heated to 105 °C, and kept to a constant mass. The most precise automatic switch-off criterion (a fixed weight loss of 1 mg per 140 s) was selected.

**Table 2**  
Conditions of the Hg  $L_{\alpha}$  line scan.

| Parameter                            | Value        |
|--------------------------------------|--------------|
| Voltage, kV                          | 60           |
| Current, mA                          | 70           |
| Prime beam filter                    | Al 0.5 mm    |
| Collimator                           | 0.25         |
| Crystal                              | LiF200       |
| Detector                             | SC           |
| Sample rotation                      | on           |
| Counting time, s                     | 4            |
| Start scan angle, 2 $\theta$ °       | 35           |
| End scan angle, 2 $\theta$ °         | 37           |
| Increment, 2 $\theta$ °              | 0.02         |
| Scan type                            | Fast digital |
| Pulse height discriminator threshold | 30           |
| Pulse height discriminator window    | 90           |

**Table 3**  
The compositions of the calibration mixtures.

| Hg content in calibration mixtures, ppm | Volume of the stock Solution 2, $\mu\text{L}$ | Volume of the stock Solution 1, $\mu\text{L}$ | $\text{SiO}_2$ weight, g |
|---|---|---|--------------------------|
| 0.01                                    | 10  | –   | 10.000                   |
| 0.05                                    | 20  | –   | 4.000                    |
| 0.10                                    | 20  | –   | 2.000                    |
| 0.20                                    | 40  | –   | 2.000                    |
| 0.40                                    | 60  | –   | 2.000                    |
| 0.60                                    | 120   | –   | 2.000                    |
| 0.80                                    | 160   | –   | 2.000                    |
| 1.00                                    | –   | 20  | 2.000                    |
| 2.00                                    | –   | 40  | 2.000                    |
| 5.00                                    | –   | 100   | 2.000                    |
| 10.0                                    | –   | 200   | 2.000                    |

### 3. Results and discussion

The analytical signal in FPAAS is the total area under the curve recorded for mercury absorption from the sample (Fig. 1A). Arbitrary units are given at the vertical axis, as peak heights do not bear any valuable analytical information in FPAAS; hence, they were normalized. The integration was carried out automatically by software. Background repeatability relative standard deviation (RSD) was no higher than 3% (see Fig. 2).

This view of a signal is caused by an increase in the concentration of mercury in the vapor when the sample was heated, but then Hg amount drops down and the signal decreases. As seen in Fig. 1 for a sample of  $\text{SiO}_2$ , where only the ionic species of Hg are presented, the peak has a unimodal shape. The same reproducible results were observed for the majority of ND samples but several samples like UDD-Alit or UDD-NanoGroup had bimodal peak shapes. This did not affect the Hg determination as the total area is used for calculations. The peaks for some of the test samples are shown in Fig. 3.

However, the peak shape gives us the additional information about Hg binding. For example, in the case of a bimodal peak, we can assume that a part of mercury binds to the ND surface stronger than the rest, which evaporates easily. If we continue to heat the sample, no new peak appears, as shown in Fig. 1B. In this experiment, we heated a RUDDM sample for 5 min and continue to measure the signal. For this time, the sample lost more than 50% of its starting weight. For comparison, the weight loss of the sample during the time when mercury evaporated was no more than 5%. This proves once again that mercury impurity is concentrated at the surface of ND crystals.

The calibration function of absorbance  $A$  vs. concentration of Hg,  $c$  (in ppm) made using Procedure 1 was linear and for the range 0–5.0 ppm is described as:

$$A = (2.90 \pm 0.03) \times 10^3 c, \quad r = 0.9997, \quad n = 31, \quad P = 0.95, \quad (1)$$

where  $r$  is the coefficient of correlation,  $n$  is the number of points in the calibration, and  $P$  is the confidence level.

A very small but readily detectable signal from  $\text{SiO}_2$  was thoroughly measured and deducted from calibration-mixture signals.

To verify the trueness of the calibration function (Eq. (1)), we analyzed a standard reference material, a soil containing  $(0.4 \pm 0.1)$  ppm of Hg. From our calculations, we obtained the value of  $(0.45 \pm 0.05)$

**Table 4**  
The compositions of ND– $\text{SiO}_2$  mixtures.

| ND product name | $\text{SiO}_2$ weight, g | ND weight, g | ND content in mixture, % | The “dilution”, times |
|-----------------|--------------------------|--------------|--------------------------|-----------------------|
| UDA-S-GO        | 1.9050                   | 0.1000       | 5.0                      | 20.1                  |
| UDA-S           | 1.9052                   | 0.1198       | 5.9                      | 16.9                  |
| UDAG-S          | 5.9070                   | 0.0960       | 1.6                      | 62.5                  |

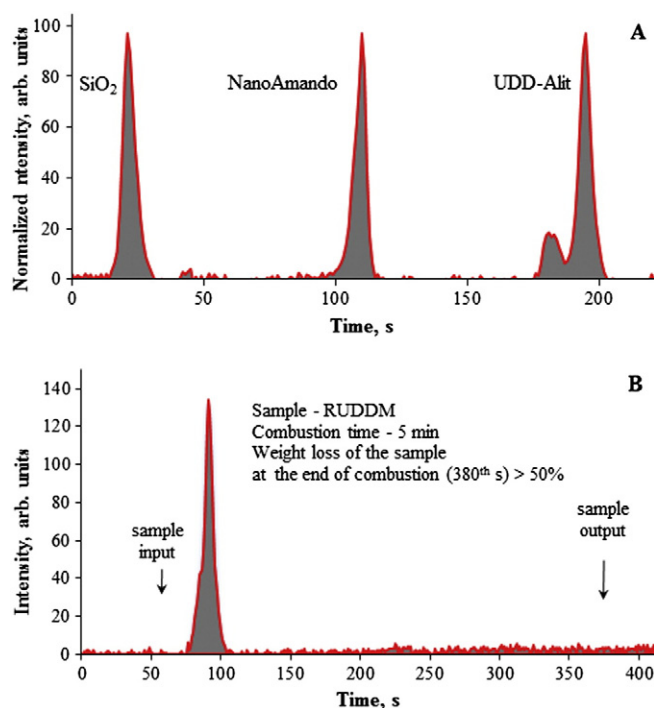


**Fig. 1.** The typical view of FPAAS absorbance curves for mercury measurements of ND samples. (A) Height-normalized peaks of different samples; (B) prolonged exposure of a RUDDM sample inside the oven with simultaneous recording of mercury absorbance; the area of the peak (the analytical signal) is shaded for convenience.

ppm. Thus, according to ISO 5725:1994 [43] we obtained a correct result.

Results obtained for ND samples from Eq. (1) and sorted by the increasing Hg content are presented in Table 5. It sums up two values for every sample: for air-dry (sample “as is” or dried at 30 °C) and absolutely dry samples. To obtain the second value, we measured the moisture content and recalculated the Hg concentration.

It is necessary to say some words about sample moisture. According to our data, the moisture of almost all samples is in the range of 2–5%. After moisture measurements, several samples were left in air and re-measured after 1 h. In this case, we obtained the same moisture values. Beside this, we observed that sample weight started increasing immediately after heating termination. Therefore, we assumed that it is physically absorbed water vapor from the surrounding air and an equilibrium value. It should be remarked that for the NanoAmando 2009 and 2012 samples we obtained water contents of  $3.0 \pm 0.1$  and  $11.8 \pm 0.3\%$ , although the manufacturer gave 25 and 20%, respectively (the so-called “hard gel” or “hydrogel” in E. Osawa’s notation [48]). This means that the “hard gel” is not stable for long storage times after

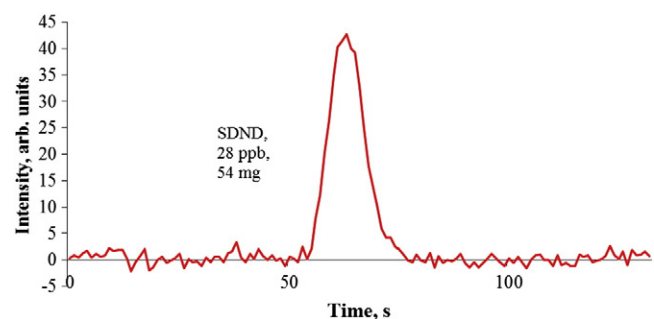


**Fig. 2.** A peak showing background fluctuations used for the measurement of the limits of quantification.

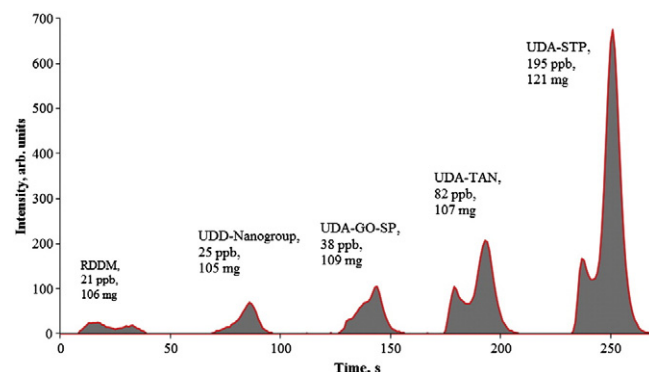


**Fig. 3.** Peak shapes of some of ND samples measured in this study, sorted by their peak areas (increasing mercury contents); the area of the peak (the analytical signal) is shaded for convenience.

opening the manufacturer’s package. Thus, we can say that absolutely dry samples and samples with excess water are very unstable. Consequently, if it is necessary to prepare ND solutions with the maximum precise weight concentration or to determine impurities with the maximum accuracy, water content should be measured and considered. Thus, we believe that both values, with and without moisture correction, are useful for ND characterization.

Anyway, for all the range of ND samples, the precision of the determination of mercury is high and at a level, which is appropriate for FPAAS. Thus, the sample preparation of ND samples for mercury determination is very simple and does not increase the determination error. As a whole, the procedure falls within the rules imposed on high-precision element analysis in high-technology materials [49].

The overall range of Hg contents in NDs is very wide: from 20 µg/kg to more than 0.7 g/kg. The most Hg contents are determined in UDAG-S type; the most mercury-free materials are RDDM. This can be results of different technology and storage conditions, and different washing procedures. Anyway, the samples UDA-S-GO, UDA-S, and UDAG-S with Hg contents over 10 ppm seem very contaminated, and their use as a ND sample should require a procedure for purification from mercury. The Hg contents in the 10 samples with the least Hg contents (the first 10

**Table 5**  
Mercury content in nanodiamond samples ( $n = 3$ ,  $P = 0.95$ ).

| ND product name        | Moisture content, wt. % | Mercury content         |                                |
|------------------------|-------------------------|-------------------------|--------------------------------|
|                        |                         | In air-dry samples, ppm | In absolutely dry samples, ppm |
| RDDM                   | $1.3 \pm 0.1$           | $0.021 \pm 0.008$       | $0.021 \pm 0.009$              |
| UDA-GO-SP-M1           | $3.6 \pm 0.1$           | $0.023 \pm 0.002$       | $0.024 \pm 0.003$              |
| UDD-NanoGroup          | $6.6 \pm 0.2$           | $0.025 \pm 0.009$       | $0.027 \pm 0.010$              |
| UDA-GO-SP-M2           | $3.5 \pm 0.2$           | $0.026 \pm 0.003$       | $0.027 \pm 0.005$              |
| UDD-Alit               | $2.3 \pm 0.2$           | $0.028 \pm 0.008$       | $0.03 \pm 0.01$                |
| SDND                   | $4.6 \pm 0.2$           | $0.028 \pm 0.004$       | $0.029 \pm 0.006$              |
| NanoAmando 2009        | $3.0 \pm 0.1$           | $0.035 \pm 0.005$       | $0.036 \pm 0.006$              |
| NanoAmando 2012        | $11.8 \pm 0.3$          | $0.035 \pm 0.003$       | $0.040 \pm 0.004$              |
| UDA-GO-SP              | $4.3 \pm 0.2$           | $0.038 \pm 0.007$       | $0.040 \pm 0.009$              |
| RUDDM 3                | $5.6 \pm 0.2$           | $0.042 \pm 0.005$       | $0.044 \pm 0.007$              |
| RUDDM 2                | $4.9 \pm 0.2$           | $0.042 \pm 0.009$       | $0.04 \pm 0.01$                |
| RUDDM non-fractionated | $5.0 \pm 0.2$           | $0.075 \pm 0.005$       | $0.079 \pm 0.008$              |
| UDA-TAN                | $2.9 \pm 0.1$           | $0.082 \pm 0.014$       | $0.09 \pm 0.02$                |
| UDA-STP                | $3.0 \pm 0.1$           | $0.195 \pm 0.007$       | $0.20 \pm 0.02$                |
| WND                    | $7.0 \pm 0.3$           | $0.24 \pm 0.07$         | $0.26 \pm 0.08$                |
| UDA-SP                 | $2.8 \pm 0.1$           | $0.46 \pm 0.06$         | $0.47 \pm 0.08$                |
| GO1                    | $5.0 \pm 0.2$           | $1.6 \pm 0.2$           | $1.7 \pm 0.3$                  |
| UDA-S-GO               | $5.0 \pm 0.2$           | $37 \pm 4^a$            | $39.2 \pm 5.7^a$               |
| UDA-S-GO               | $5.0 \pm 0.2$           | $42 \pm 2^b$            | $45 \pm 4$                     |
| UDA-S                  | $4.9 \pm 0.2$           | $126 \pm 15^b$          | $132 \pm 21$                   |
| UDAG-S                 | $2.2 \pm 0.1$           | $717 \pm 30^b$          | $733 \pm 50$                   |

<sup>a</sup> This value was calculated from the extrapolation of the calibration function.

<sup>b</sup> Samples were diluted with SiO<sub>2</sub> as described in the text.



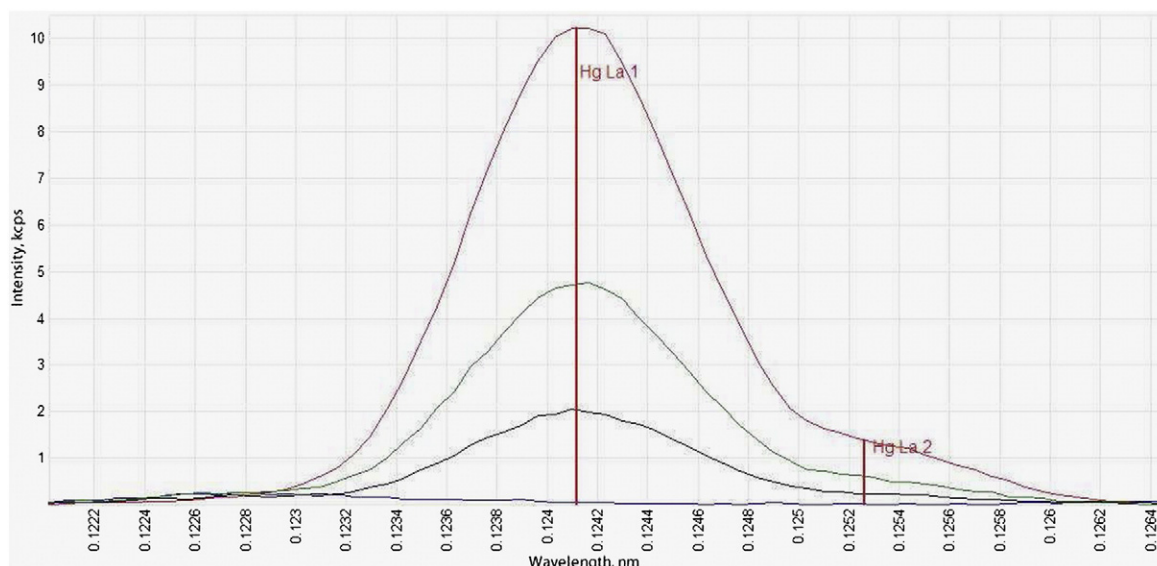


**Fig. 4.** Hg  $L_{\alpha}$  lines for nanodiamond samples: RUDDM non-fractionated (blue), UDA-S-GO (black), UDA-S (green), UDA-S (red). See Table 2 for the measurement conditions. The figure was directly exported from OXSAS software (Thermo Scientific). Intensity is given in kilo-counts per second (kcps).

lines in Table 5) show that the Hg concentrations in these samples are statistically insignificant from each other, and the average Hg concentration for these samples is  $(0.03 \pm 0.02)$  ppm.

To prove the results for FPAAS, we checked the mercury concentration in selected ND samples (with high concentrations of Hg obtained using FPAAS) with wavelength-dispersive XRF. In all the selected samples, we obtained strong, reliably identified, and reproducible peaks of Hg (see Fig. 4). Peak heights are in good concordance with the Hg values from FPAAS measurements. Nevertheless, the accuracy of quantitative XRF determination of Hg in NDs was far beyond the scope of this manuscript and is a theme for a separate research, so we used XRF here for qualitative confirmation of our results only. Quantitative comparison of FPAAS and ICP-AES data for samples UDA-S-GO, UDA-S, and UDA-S can be found in [29].

#### 4. Conclusions

Thus, our study shows that the amounts of Hg in NDs are very different depending on the product name and manufacturer. So a wide range is not expected from the technology conditions, but these results confirmed the necessity to control Hg content in NDs. Taking in the values, 120 and especially 700 ppm (0.7 g Hg per kg of NDs) are very high indeed. Such a Hg level can be dangerous not only for cell cultures in biological experiments, but even also for people working with this material in the industry. Nowadays, there are no standards on tolerance quantities of mercury in NDs, and this study shows that working out such a standard or at least a regulation is topical. As the results of this study show, that the precision of flameless pyrolysis atomic absorption determination of mercury in nanodiamonds is high, this method can be recommended as a basic method for routine Hg measurements in nanodiamonds.

#### Prime novelty statement

The first time mercury was determined in nanodiamonds, the total mercury was determined in 20 samples of various manufacturers, which provides a survey of mercury with a very wide range of concentrations.

#### Acknowledgments

We are grateful to Professor Eiji Osawa (NanoCarbon Research Institute Co. Ltd., Japan) for providing NanoAmando samples and Dr. Vladimir I. Padalko (ALIT, Kiev, Ukraine and NanoGroup Co., Prague, Czech Republic) for providing UDD-Alit and UDD-Nanogroup samples. This work was supported by RFBR grant 13-03-00535a. This work was supported in part (a Thermo Scientific ARL Advant'x 4200 XRF spectrometer) by M.V. Lomonosov Moscow State University Program of Development.

#### References

- [1] D. Ho, in: Springer, New York, Dordrecht, Heidelberg, London, 2010, pp. 304.
- [2] O.V. Turova, E.V. Starodubtseva, M.G. Vinogradov, V.I. Sokolov, N.V. Abramova, A.Y. Vul, A.E. Alexenskiy, Catal. Commun. 12 (2011) 577–579.
- [3] N.N. Vershinin, O.N. Efimov, V.A. Bakaev, A.E. Aleksenskii, M.V. Baidakova, A.A. Sitnikova, A.Y. Vul, Fullerenes Nanotubes Carbon Nanostruct. 19 (2011) 63–68.
- [4] V.S. Bondar, I.O. Pozdnyakova, A.P. Puzyr, Phys. Solid State 46 (2004) 758–760.
- [5] S.-Y. Wu, W.-M. Chang, H.-Y. Tseng, C.-K. Lee, T.-T. Chi, J.-Y. Wang, Y.-W. Kiang, C.C. Yang, Plasmonics 6 (2011) 547–555.
- [6] N.A. Skorik, A.L. Krivozubov, A.P. Karzhenevskii, B.V. Spitsyn, Prot. Met. Phys. Chem. Surf. 47 (2011) 54–58.
- [7] G.P. Bogatyreva, M.A. Marinich, V.L. Gvyazdovskaya, Diamond Relat. Mater. 9 (2000) 2002–2005.
- [8] B.R. Smith, D.W. Inglis, B. Sandnes, J.R. Rabeau, A.V. Zvyagin, D. Gruber, C.J. Noble, R. Vogel, E. Osawa, T. Plakhotnik, Small 5 (2009) 1649–1653.
- [9] N. Mohan, Y.-K. Tzeng, L. Yang, Y.-Y. Chen, Y.Y. Hui, C.-Y. Fang, H.-C. Chang, Adv. Mater. 22 (2010) 843–847.
- [10] N. Mohan, C.-S. Chen, H.-H. Hsieh, Y.-C. Wu, H.-C. Chang, Nano Lett. 10 (2010) 3692–3699.
- [11] M. Chen, X.-Q. Zhang, H.B. Man, R. Lam, E.K. Chow, D. Ho, J. Phys. Chem. Lett. 1 (2010) 3167–3171.
- [12] M. Chen, E.D. Pierstorff, R. Lam, S.-Y. Li, H. Huang, E. Osawa, D. Ho, ACS Nano 3 (2009) 2016–2022.
- [13] L. Tang, C. Tsai, W.W. Gerberich, L. Kruckeberg, D.R. Kania, Biomaterials 16 (1995) 483–488.
- [14] S. Kelly, E.M. Regan, J.B. Uney, A.D. Dick, J.P. McGeehan, E.J. Mayer, F. Claeysens, Biomaterials 29 (2008) 2573–2580.
- [15] Y.-C. Chen, D.-C. Lee, T.-Y. Tsai, C.-Y. Hsiao, J.-W. Liu, C.-Y. Kao, H.-K. Lin, H.-C. Chen, T.J. Palathinkal, W.-F. Pong, N.-H. Tai, I.N. Lin, I.-M. Chiu, Biomaterials 31 (2010) 5575–5587.
- [16] L. Kuang-Kai, et al., Nanotechnology 18 (2007) 325102.
- [17] K.-K. Liu, C.-C. Wang, C.-L. Cheng, J.-I. Chao, Biomaterials 30 (2009) 4249–4259.
- [18] A.P. Puzyr, D.A. Neshumayev, S.V. Tarskikh, G.V. Makarskaya, V.Y. Dolmatov, V.S. Bondar, Diam. Relat. Mater. 13 (2004) 2020–2023.
- [19] S. Vial, C. Mansuy, S. Sagan, T. Irinopoulou, F. Burlina, J.-P. Boudou, G. Chassaing, S. Lavielle, ChemBioChem 9 (2008) 2113–2119.

- [20] V.Y. Dolmatov, *Russ. Chem. Rev.* 70 (2001) 607.
- [21] A.L. Vereshchagin, *Svoistva detonatsionnykh nanoalmazov* (Properties of Detonation Nanodiamonds), Izdatel'stvo Altaiskogo Universiteta, Barnaul, 2005.
- [22] B.V. Spitsyn, M.N. Gradoboev, T.B. Galushko, T.A. Karpukhina, N.V. Serebryakova, I.I. Kulakova, N.N. Melnik, Purification and Functionalization of Nanodiamond, in: D. Gruen, O. Shenderova, A. Vul' (Eds.), *Synthesis, Properties and Applications of Ultrananocrystalline Diamond*, Springer Netherlands, 2005, pp. 241–252.
- [23] G.P. Bogatyreva, M.A. Marinich, E.V. Ishchenko, V.L. Gvyazdovskaya, G.A. Bazalii, *J. Superhard Mater.* (2002) 10–15.
- [24] Y.W. Zhu, X.Q. Shen, Z.J. Feng, X.G. Xu, B.C. Wang, *J. Mater. Sci. Technol.* 20 (2004) 469–471.
- [25] O.A. Shenderova, D.M. Gruen, in: William Andrew Publishing, Norwich, New York, U.S.A., 2006, pp. 624.
- [26] G.P. Bogatyreva, M.A. Marinich, V.Y. Zabuga, G.G. Tsapyuk, A.N. Panova, G.A. Bazalii, *J. Superhard Mater.* 30 (2008) 305–310.
- [27] G.P. Bogatyreva, V.Y. Zabuga, G.G. Tsapyuk, A.N. Kuzmich, *Rock Cutting and Metal-machining Tools — Machinery and Technology of its Production and Application: Proceedings*, 2004. 107–110.
- [28] D.P. Mitev, A.T. Townsend, B. Paull, P.N. Nesterenko, *Carbon* 60 (2013) 326–334.
- [29] D.S. Volkov, M.A. Proskurnin, M.V. Korobov, *Carbon* 74 (2014) 1–13.
- [30] W.L. Clevenger, B.W. Smith, J.D. Winefordner, *Crit. Rev. Anal. Chem.* 27 (1997) 1–26.
- [31] E.C. Magalhaes, A.H. Fostier, H. Berndt, *J. Anal. At. Spectrom.* 12 (1997) 1231–1234.
- [32] C.T. Costley, K.F. Mossop, J.R. Dean, L.M. Garden, J. Marshall, J. Carroll, *Anal. Chim. Acta.* 405 (2000) 179–183.
- [33] G.E.M. Hall, P. Pelchat, *Analyst* 122 (1997) 921–924.
- [34] A.A. Ganeev, S.E. Pogarev, V.V. Ryzhov, S.E. Sholupov, T.V. Dreval, *Ecol. Chem. (Russ.)* 4 (1995) 122–126.
- [35] J.W. Robinson, E.M. Skelly, *Spectrosc. Lett.* 14 (1981) 519–551.
- [36] S.E. Pogarev, V.V. Ryzhov, N.R. Mashyanov, M.B. Sobolev, *Water Air Soil Pollut.* 97 (1997) 193–198.
- [37] G. Jarzynska, J. Falandysz, *J. Environ. Sci. Health. Part A Toxic/Hazard. Subst. Environ. Eng.* 46 (2011) 569–573.
- [38] C. Bin, W. Xiaoru, F.S.C. Lee, *Anal. Chim. Acta.* 447 (2001) 161–169.
- [39] S. Pogarev, V. Ryzhov, N. Mashyanov, S. Sholupov, V. Zharskaya, *Anal. Bioanal. Chem.* 374 (2002) 1039–1044.
- [40] Y.M. Panta, S. Qian, C.L. Cross, J.V. Cizdziel, *J. Anal. Appl. Pyrolysis* 83 (2008) 7–11.
- [41] ISO/IEC 17025:2005, General Requirements for the Competence of Testing and Calibration Laboratories, ISO/IEC, 2005.
- [42] IUPAC, Stability Constant Database, Royal Society of Chemistry, SCQuery, Version 1. 381994.
- [43] ISO 5725:1994, (Revised and confirmed in 2012): accuracy (trueness and precision) of measurement methods and results, 1994.
- [44] S.E. Sholupov, A.A. Ganeyev, *Spectrochim. Acta B Atomic Spectrosc.* 50 (1995) 1227–1236.
- [45] S.E. Sholupov, A.A. Ganeev, A.D. Timofeev, V.M. Ivankov, *J. Anal. Chem.* 50 (1995) 589–594.
- [46] A. Ganeev, S.E. Sholupov, M.N. Slyadnev, *J. Anal. Chem.* 51 (1996) 788–796.
- [47] Y. Jung, R. Reif, Y. Zeng, R.K. Wang, *Nano Lett.* 11 (2011) 2938–2943.
- [48] M.V. Korobov, N.V. Avramenko, A.G. Bogachev, N.N. Rozhkova, E. Ōsawa, *J. Phys. Chem. C* 111 (2007) 7330–7334.
- [49] J. Inczedy, *IUPAC Compendium of Analytical Nomenclature*, Blackwell Scientific Publications, 1998.